Resbee Publishers

Multimedia Research (MR)

Received 18 December, Revised 26 February, Accepted 27 March

Hybrid classifier: Brain Tumor Classification and Segmentation using Genetic-based Grey Wolf optimization

Avinash Gopal
Research on Artificial Intelligence and Smart Assistants,
RWTH Aachen University, 52062 Aachen, Germany
avinashgopal321@gmail.com

Abstract: This work uses a novel brain tumor classification technique which comprises 5 steps like "(i) denoising, (ii) skull stripping, (iii) segmentation, (iv) feature extraction and (v) classification". At first, the image is given in the denoising procedure, whereas the amputation of the noise process is performed by using an entropy-oriented trilateral filter. Subsequently, noise removed image is used to skull stripping procedure through morphology segmentation and Otsu thresholding. Then, the segmentation takes place using the adaptive CLFAHE method. GLCM features are extracted after finishing segmentation. Here, hybrid classification represents the hybridization of 2 classifiers such as FNN and "Bayesian regularization classifier". The very important involvement lies in the best selecting of hidden neurons in FNN. In this paper, a novel genetic algorithm based GWO (GA-GWO) method is proposed that hybrids the conception. At last, the proposed method performance is evaluated with conventional techniques to show the supremacy of the proposed method.

Keywords: Brain Tumour; GLCM; FNN; Fuzzy Logic; Optimization Algorithm

Nomenclature

Abbreviations	Descriptions
CLFAHE	Contrast Limited Fuzzy Adaptive Histogram Equalization
FNN	Feedforward neural network
GLCM	Gray-level cooccurrence matrix
FNR	False-negative rate
ROI	Region of Interest
NPV	Negative Predictive Value
CT	Computed Tomography
MCC	Matthews correlation coefficient
FPR	False-positive rate
WPTE	Wavelet Packet Tsallis Entropy
FDR	False Discovery Rate
CNN	Convolutional Neural Network
SVM	Support Vector Machine
ST	Scattering Transform
LGG	Lower-Grade Glioma
FLAIR	Fluid Attenuated Inversion Recovery
GWO	Grey Wolf optimization
DAC	Deep Autoencoder
PRI	Raspberry Pi
ML	Machine Learning
MRI	Magnetic Resonance Imaging
BFC	Bayesian fuzzy clustering
JOA	Jaya optimization algorithm
BTS	Brain Tumor Segmentation
FRFCM	Fast and Robust Fuzzy C-Means Clustering
NN	Neural Network
MSE	Mean Squared Errors
ELM	extreme learning machine

https://doi.org/10.46253/j.mr.v3i2.a1

1. Introduction

Image classification and the segmentation is the important image processing algorithms exploited to segment the ROI and to classify them into the given classes. Image classification and the segmentation play a very important function for numerous applications inconsiderate images, feature extraction, interpreting and analyzing them [2]. It encompasses widespread application in brain imaging, for instance, tissue classification, volume estimation of the tumor, tumor position, blood cell demarcation, planning of surgical, matching. CT and MRI scan is exploited to resects and inspect the aberration in stipulations of size, shape, else position of tissues in the brain. In Brain, Brain Tumor is a neoplastic and atypical cell growth. Also, Brain tumors called neoplasia or lesion can be mostly classified into Primary and Metastatic tumors [1]. From brain tissues, primary brain tumor instigates and its background.

Generally, intracranial tumors, called as brain tumors are considered as fatal cancers. Primary recognition of brain tumors is essential that can progress treatment likelihood and augment the patient's survival rate. Medical imaging presents technical maintain for premature identifying brain tumors. In these imaging techniques, MRI not only presents better contrast for brain soft tissues and multi-azimuth imaging however it is a radiation-free and non-invasive method. It turns out to be well-liked analytical equipment for brain tumors [5]. During the therapies for defensive healthier tissues except for harmful tumor cells, it is vital to segment them. Nevertheless, it is not practical to interpret and segment a great quantity of MRI physically that is an extremely time-consuming task and congestion to the physician [1].

Exploiting MRI there are more than a few techniques for usual tumor segmentation which is chiefly based on the discriminative or generative techniques. Generative techniques like atlas-based techniques necessitate prior knowledge of anatomy, also, to employ posterior probabilities for voxels' classification attended for tumor segmentation by image registration [6]. Conversely, discriminative techniques like machine learning-based SVM. Dimensionality minimization and a selection of imaging features are typically implemented previously to the training model. In addition, CNN shows a potential ML technique which is diverse from distinctive techniques, and extraction, is automated through model training and has demonstrated assure an automatic tumor segmentation [16] [17] [18] [19].

The superiority of the meta-heuristic approaches can be necessary during their applicability that is they have been used to some difficulty formulation as function optimization issues; hybridization that is these techniques has been integrated to structure additional vigorous methods; flexibility that is these techniques has been scaled consistently with the issue.

The main intention of the paper is to present a novel brain tumor classification model. Here, the entropy-based trilateral filter is examined to perform denoising procedure. Moreover, the subsequent phase is skull striping which is the procedure by exploiting morphology segmentation and Otsu thresholding. Consequently, the segmentation is done exploiting the Adaptive CLFAHE model. After that, as per GLCM the features are extracted and given to hybrid classifiers. The most important objective of this paper is the improvement of classification rate using optimization theory through choosing the best-hidden neurons of the FNN method. For this, a novel approach is proposed called GA-GWO that covers for improved classification rate. Ultimately, the proposed technique and existing techniques are evaluated regarding the performance metrics and the outcome is investigated.

2. Literature Review

In 2020, Mostefa Ben naceur et al [1], presented a new Deep CNNs enthusiastic to completely automatic segmentation of Glioblastoma brain tumors about low- and high-grade. The proposed CNN's technique was enthused by the Occipito-Temporal pathway that had an individual function named selective attention which exploits diverse accessible sizes of the field in consecutive layers to understand the vital objects in a prospect. Hence, from MRI images, selective attention technique was exploited to widen CNN's method aids to exploit extraction for significant features.

In 2020, Mohamed A. Naser and M. Jamal Deen [2], proposed a deep learning technique which integrates CNN based on the U-net for segmenting tumor and transport learning. The segmentation and grading techniques employs a similar pipeline of T1-precontrast, FLAIR, and T1-postcontrast MRI images of LGG for training and estimation for 110 patients.

In 2019, Raja and rani [3], proposed a classification approach for brain cancer by exploiting the "Bayesian fuzzy clustering" oriented segmentation technique. At first, the images were pre-processed for denoising reasons by exploiting the non-local mean filter. Subsequently, the BFC method was used for the brain tumors segmentation. After segmentation, vigorous features like ST information-theoretic measures, and WPTE techniques were exploited for the feature extraction procedure. At last, a hybrid method of DAE based JOA by means of a softmax regression.

In 2019, Arti Tiwari et al [4], provided a methodical literature review of methods for brain tumor classification and segmentation of normality and abnormality from MRI images based on the diverse techniques such as metaheuristic methods, deep learning methods, and hybridization of these two. It integrates the production and quantitative analysis from the existing segmentation and classification methods of finest in class schemes.

In 2019, Fatih Ş İ Ş İK and Eser Sert [5], proposed, a BTS technique based on ELM and significantly FRFCM methods running on PRI hardware. The current research mostly aspires to initiate a novel segmentation system hardware comprising novel techniques and presenting a higher accurateness. PRI's were helpful cellular device because of its cost-efficiency and fulfilling hardware.

In 2019, Zexun Zhou et al [6] exploited 3D atrous-convolution to restore striding and construct the backbone for feature learning. A "3D atrous-convolution feature pyramid" was modeled and augmented to the conclusion of the backbone for the next issue. This construction enhances the discriminating capability of the large technique to segment tumors with diverse sizes by combining with contextual features.

3. Hybridization Model: Proposed Brain Tumor Classification Technique

The most important contribution of this work is to develop a model for brain cancer classification which overwhelms the accurateness issues in MRI. The proposed technique comprises several phases like "denoising, skull stripping, feature extraction, segmentation, and classification". The gradual demonstration of these procedures is described as below:

The primary procedure includes the image denoising and it is used by deploying the entropy-based bilateral filter procedure. Formerly after the conclusion of the denoising procedure, the image is fed to the skull stripping procedure that is holded exploiting the morphology segmentation and Otsu thresholding methods. Moreover, the subsequent phase is the segmentation process and it is entrenched to segment image after the skull stripping procedure. This is carried out using the Adaptive CLFAHE model. Previously the segmentation procedure gets finished; GLCM based feature extraction is done. At last, image classification is performed exploiting the novel hybridized model that is the integration of DBN and the Bayesian network. The optimization conception is included in this classification procedure, it refers to hidden neurons of the DBN technique and the membership function of fuzzy logic is chosen optimally exploiting GA-GWO. The classification procedure endowments classified results.

3.1 Denoising Model

At first, from the original image, the image is subjected to a denoising procedure, whereas the noise is evaded. For this reason, an entropy-based bilateral filter [7] model is exploited. This procedure is described below:

Entropy-based Bilateral Filter: The inspiration of this Entropy filter is the bilateral filter which is the integration of range filtering and a domain for edge protection. A novel range filter is done that is the integration of adaptive median filter in weighting function is presented using the Eq. (1). Moreover, the median metric module is indicated as $We^{M}_{\theta_{\hat{x}},\vartheta_{\hat{y}}}$, from a median intensity attained exploiting the enhanced adaptive median filter initializing up to a maximum of $(2L+1)^2$ a neighbourhood of resulting location is shown by $J^{M}(.,.)$. In photographic images, entropy function is stated as eq. (2). Moreover, eq. (3) presents probability at $\mu_{\hat{x}},\mu_{\hat{y}}$, whereas, the disparity between J and J^{M} is indicated as $E(\mu_{\hat{x}},\mu_{\hat{y}})$ in Eq. (4). Moreover, the absolute value is indicated in $|.|$ and the utmost probable value of the pixel is stated as J_{max}. The weights are altered between radiometric and median-metric models exploiting the entropy function En and it are shown in eq. (5). Finally, the weighting of J^{M} is presented in Eq. (6), and attains the denoised image.

$$We^{M}_{\theta_{\hat{x}},\vartheta_{\hat{y}}} = \exp\left[-\frac{\left|J^{M}(\mu_{\hat{x}},\mu_{\hat{y}}) - J^{M}(\theta_{\hat{x}},\theta_{\hat{y}})\right|^2}{2\sigma_M^2}\right] \tag{1}$$

$$\begin{aligned} En\left(\theta_{\hat{x}},\theta_{\hat{y}}\right) = &- \sum_{(\mu_{\hat{x}},\mu_{\hat{y}})\in\Psi\left(\theta_{\hat{x}},\theta_{\hat{y}}\right)} pr(\mu_{\hat{x}},\mu_{\hat{y}})\log pr(\mu_{\hat{x}},\mu_{\hat{y}}) \\ &+ [1-pr(\mu_{\hat{x}},\mu_{\hat{y}})]\log[1-pr(\mu_{\hat{x}},\mu_{\hat{y}})] \end{aligned} \tag{2}$$

$$pr(\mu_{\hat{x}},\mu_{\hat{y}}) = \frac{[1-E(\mu_{\hat{x}},\mu_{\hat{y}})]^2}{2} + 0.5 \tag{3}$$

$$E(\mu_{\hat{x}},\mu_{\hat{y}}) = \frac{\left|J(\mu_{\hat{x}},\mu_{\hat{y}}) - J^M(\mu_{\hat{x}},\mu_{\hat{y}})\right|}{J_{max}} \tag{4}$$

$$We'_{\theta_{\hat{x}},\theta_{\hat{y}}} = We^S{}_{\theta_{\hat{x}},\theta_{\hat{y}}} (We^L{}_{\theta_{\hat{x}},\theta_{\hat{y}}})^{\frac{2}{2+En(\theta_{\hat{x}},\theta_{\hat{y}})}} (We^M{}_{\theta_{\hat{x}},\theta_{\hat{y}}})^{En(\theta_{\hat{x}},\theta_{\hat{y}})} \tag{5}$$

$$J'_{\theta_{\hat{x}},\theta_{\hat{y}}} = \frac{\sum_{(\mu_{\hat{x}},\mu_{\hat{y}})\in\Psi} We'_{\theta_{\hat{x}},\theta_{\hat{y}}}(\mu_{\hat{x}},\mu_{\hat{y}}) J^M(\mu_{\hat{x}},\mu_{\hat{y}})}{\sum_{(\mu_{\hat{x}},\mu_{\hat{y}})\in\Psi} We'_{\theta_{\hat{x}},\theta_{\hat{y}}}(\mu_{\hat{x}},\mu_{\hat{y}})} \tag{6}$$

3.2 Skull Stripping model

Here, denoised images are subjected to input and procedure is performed by organized morphology segmentation and Otsu thresholding. These procedures are explained as below:

Otsu Thresholding: It is an algorithm [8] which represents image encompasses only background and the object in addition to it communicates to linear discriminant criterion. By the Otsu, the value of the threshold is set, and thus minimizes overlapping in class distributions. Hence, image is segmented into 2 features dark and light regions $T0$ and $T1$, where the level of intensity series from 0 to th ($T0 = (0,1,....,th\}$, $T1 = (th, th+1,....,\bar{l}-1,\bar{l}\}$), whereas the value of the threshold is stated by th and image utmost grey level is stated as 1. The object can allocate about $T0$ and $T1$ or simultaneously. The complete probable values of the threshold are scanned by this and estimation of the minimized pixel-level value. The value of threshold with the least amount of entropy is the most important objective of this Otsu thresholding. This procedure is described as follows. Let the histogram probability for experiential gray value as $hp(\bar{i})$, $\bar{i} = 1,....., \bar{l}$.

Moreover, the index image for the column and a row is stated as $\bar{r}$ and $\bar{c}$, respectively, and the number of columns and rows of the image is shown by $\bar{R}$ and $\bar{C}$, respectively.

The mean, weight, and class variance $T0$ with the value of intensity which lies among 0 to th, is offered by $\mu_{\bar{b}}(th)$, $\omega_{\bar{b}}(th)$, and $\sigma_{\bar{b}}(th)$, correspondingly. The mean, weight, and class variance $T1$ with the value of intensity are denoted by $\omega_{\bar{f}}(th)$, $\sigma_{\bar{f}}(th)$ and $\mu_{\bar{f}}(th)$, correspondingly. The weighted sum of cluster variation is shown as σ^2_{ω}.

The value using the least lass variance is presumed as the optimal value of the threshold $th*$. The subsequent eq. (8) presents within-class variance.

$$hp(\bar{i}) = \frac{no\{(\bar{r},\bar{c})\left|image\ (\bar{r},\bar{c}) = \bar{i}\right.\}}{\bar{R}.\bar{C}} \tag{7}$$

$$\sigma^2_{\omega} = \omega_{\bar{b}}(th) * \sigma^2_{\bar{b}}(th) + \omega_{\bar{f}}(th) * \sigma^2_{\bar{f}}(th) \tag{8}$$

$$\text{where, } \omega_{\bar{b}}(th) = \sum_{\bar{i}=1}^{th} hp(\bar{i}) \tag{9}$$

$$\omega_{\bar{f}}(th) = \sum_{\bar{i}=th+1}^{\bar{l}} hp(\bar{i}) \tag{10}$$

$$\mu_{\bar{b}}(th) = \frac{\sum_{\bar{i}=1}^{th} \bar{i} * hp(\bar{i})}{\omega_{\bar{b}}(th)} \tag{11}$$

$$\mu_{\bar{f}}(th) = \frac{\sum_{\bar{i}=th+1}^{\bar{l}} \bar{i} * hp(\bar{i})}{\omega_{\bar{f}}(th)} \tag{12}$$

$$\sigma^2_{\bar{b}}(th) = \frac{\sum_{\bar{i}=1}^{th} (\bar{i} - \mu_{\bar{b}}(th))^2 * hp(\bar{i})}{\omega_{\bar{b}}(th)} \tag{13}$$

$$\sigma^2_{\bar{f}}(th) = \frac{\sum_{\bar{i}=th+1}^{\bar{l}} (\bar{i} - \mu_{\bar{f}}(th))^2 * hp(\bar{i})}{\omega_{\bar{f}}(th)} \tag{14}$$

Morphology Segmentation: These morphology operations are mostly based on set theory and mainly of them are logical operations that are easier to exploit. In particular, dilation and erosion are the two fundamental morphological operations. Based on the two operations, the opening operation is estimated.

Opening: The process of erosion and dilation is indicated as the image opening. The element $\tilde{B}$ which models the image opening $\tilde{A}$ is stated exploiting eq. (15).

$$\tilde{A} \circ \tilde{B} = (\tilde{A} \Theta \tilde{B}) \oplus \tilde{B} \tag{15}$$

The relationship between erosion, opening, and dilation, is stated in Eq. (1).

The opened boundary of the image is deliberated as $\tilde{B}$ that attains tremendous points of bounds of $\tilde{A}$ and $\tilde{B}$ is "rolled" approximately in this bounds.

4. Feature Extraction: GLCM based Features

4.1 Feature Extraction using GLCM

Previously the image segmentation is finished, GLCM [9] based feature extraction is performed and it is stated as below:

Grey-Level Co-occurrence Matrix: The spatial correlation between the two pixels at the direction angle and accurate distance is done by taking into consideration of the GLCM texture. In general, a matrix co-occurrence is created exploiting this GLCM in an image data, by that matrix function characteristics can be obtained. The GLCM properties are stated as below:

Contrast: This is also called a sum of squares variance that is the intensity contrast's estimation between the pixel and its neighbor in the complete image. Eq. (16) presents the computation of contrast.

$$\text{Contrast} = \sum_{\hat{p},\hat{q}=1}^{\overline{N}} MA_{\hat{p},\hat{q}} (\hat{p} - \hat{q})^2 \tag{16}$$

Energy or Uniformity: It indicates the measure to analyze gray-level intensity concentration in GLCM. In the GLCM sum of squared elements is returned by this. The computation of energy value is done indicated as Eq. (17).

$$\text{Energy} = \sum_{\hat{p},\hat{q}=1}^{\overline{N}} MA_{\hat{p},\hat{q}}{}^2 \tag{17}$$

Homogeneity: The homogeneity is calculated using the Eq. (18).

$$\text{Homogeneity} = \frac{\sum_{\hat{p},\hat{q}=1}^{\overline{N}} MA_{\hat{p},\hat{q}}}{1 + (\hat{p} - \hat{q})^2} \tag{18}$$

Correlation: The correlation value computation is done using Eq. (19), whereas, the variance and mean are decided using the Eq. (20) and (21).

$$\text{Correlation} = \sum_{\hat{p},\hat{q}=1}^{\overline{N}} \frac{(\hat{p} - \mu_{\hat{p}})(\hat{q} - \mu_{\hat{q}})}{\sigma_{\hat{p}} \sigma_{\hat{q}}} MA_{\hat{p},\hat{q}} \tag{19}$$

$$\begin{aligned} \sigma_{\hat{p}} &= \sum_{\hat{p}=1}^{\overline{m}} (\hat{p} - \mu_{\hat{p}})^2 \sum_{\hat{q}=1}^{\overline{m}} MA_{\hat{p},\hat{q}} \\ \sigma_{\hat{q}} &= \sum_{\hat{q}=1}^{\overline{m}} (\hat{q} - \mu_{\hat{q}})^2 \sum_{\hat{p}=1}^{\overline{m}} MA_{\hat{p},\hat{q}} \end{aligned} \tag{20}$$

$$\mu_{\hat{p}} = \sum_{\hat{p}=1}^{\overline{m}} \hat{p} \sum_{\hat{q}=1}^{\overline{m}} MA_{\hat{p},\hat{q}}, \quad \mu_{\hat{q}} = \sum_{\hat{q}=1}^{\overline{m}} \hat{q} \sum_{\hat{p}=1}^{\overline{m}} MA_{\hat{p},\hat{q}} \tag{21}$$

whereas, the vertical and horizontal coordinates matrix is indicated as $\hat{p}$ and $\hat{q}$, and the matrix values in $\hat{p}$ and $\hat{q}$ coordinates is stated as $MA_{\hat{p},\hat{q}}$. Ultimately, from the image, the features are extracted during the feature extraction procedure.

4.2 Adaptive CLFAHE Segmentation

In this work, segmentation takes place using a novel Adaptive CLFAHE method [10].

5. Brain Tumor Classification: Proposed Hybrid Classifier and optimization algorithms

The classification procedure using a hybrid technique is done after the extracted features. The extracted or attained features are subject to the input to a hybridized classifier. The processes of Bayesian classifier and FNN are described as follows:

5.1 Bayesian Regularization[BR]

BR [11] is represented as a regularization method about the capability to gain lower MSE. In the BR network, the objective model and secondary term are increased by the regularization to penalize enormous weights to achieve higher smoother mapping. The gradient-based optimization method is organized to minimize the objective model which is stated in Eq. (22).

$$H = \beta K_V(I \mid W, N) + \alpha K_U(W \mid N) \tag{22}$$

In eq. (22), $K_U(W \mid N)$ is $K_U = \frac{1}{g}\sum_{c=1}^{g} W_c^2$, the "augmented squares of network weights α and β are deliberated as hyperparameters, K_V indicates the mean summation of network square error, $\alpha K_U(W \mid N)$ is called as weight decay, and α indicates decay rate". While $\alpha << \beta$ the error is minimized else, the weight size is minimized. The Bayes rule updates posterior weight distribution PD and which is shown in Eq. (23), whereas $PD(W \mid \alpha, N)$ and $PD(P \mid W, \beta, N)$ indicates the prior distribution of weight and likelihood function.

$$PD(W \mid P, \alpha, \beta, N) = \frac{PD(P \mid W, \beta, N) PD(W \mid \alpha, N)}{PD(P \mid \alpha, \beta, N)} \tag{23}$$

Using the optimized weight the posterior probability of W is increased which can be similar to the reduction of the objective function $O_B = \beta K_V + \alpha K_U$.

In the theory of Mackay, Eq. (22) is recognized exploiting the Eq. (24), whereand y indicates scrutiny number and entire network constraints, respectively. Eq. (24) states Eq. (25), where the objective model Hessian matrix is indicated as H^{MAP} well as MAP is extended as 'Maximum A Posteriori.'

$$\begin{aligned} PD(P \mid \alpha, \beta, N) &= \frac{PD(P \mid W, \beta, N) PD(W \mid \alpha, N)}{PD(W \mid P, \alpha, \beta, N)} \\ &= \frac{Z_{O_B}(\alpha, \beta)}{(\pi/\beta)^{x/2}(\pi/\alpha)^{y/2}} \end{aligned} \tag{24}$$

$$Z_{O_B}(\alpha, \beta) = \infty \mid H^{MAP} \mid^{-\frac{1}{2}} \exp\left(-O_B\left(W^{MAP}\right)\right) \tag{25}$$

Eq. (26) indicates the parameter updating at t iteration, whereas, the damping factor of Levenberg is shown as μ, the jacobian matrix is stated as J. In addition, μ is adjustable for complete iterations.

$$W^{q+1} = W^q - \left[I^T I + \mu P\right]^{-1} I^T e \tag{26}$$

In this, the output of DBN and Bayesian regularization is taken and carries out "OR" operation. The ensuing result is represented as a classification result.

5.2 FNN

In feed-forward neural networks (FNNs), previous layer neurons are completely linked to the succeeding layer, when no intra-layer associations are recognized. FNNs are expansively used in trend prediction, image classification, scene labeling, and other applications. At present, one more mainly well-liked FNNs application is represented as concluding output layer of CNNs, whereas "superior-level feature extraction is attained by pooling layers, convolutional layers, and normalization layers". For classification, softmax and ReLU is extensively exploited for intermediary classification of images. In [15], stage function ReLUs significantly accelerates convergence over tanh and sigmoid functions because of its linear model. Moreover, ReLUs used in these networks based on the training procedure. A characteristic mathematical formulation is represented as follows:

$$y_i = \max\left(0, \sum_j w_{ij} y_j\right) \tag{27}$$

In eq. (27), w_{ij} indicates the weight connecting unit; y_i indicates the activation of unit i, j indicates the prior layer to i a present layer, and y_j indicates activation of j in the previous layer. y_i indicates synaptic current input created by its pre-synaptic.

5.3 Conventional GWO

Grey Wolf Optimization (GWO) is considered as the biologically enthused optimization method exploited in several fusion applications [12]. The GWO approaches emulate the grey wolf family hunting nature. In GWO, the optimal wolf named α are leading wolves in the pack. In a hierarchy, second optimal named β, they are subsidiary to α wolves. If α wolves are nonattendance in pack subsequently β wolves can guide pack. The wolves with the least ranking are named ω. The remaining wolves are named as δ. The δ wolves require obeying α and β level wolves other than controlling over ω wolves in their pack [13].

The GWO approach arithmetical modelling comprises of 3 phases, encircling, tracking, and attacking prey [13]. The numerical model to encircle the prey is represented in below formulations:

$$\vec{D} = |\vec{C} \cdot \vec{Y}_{p_t} - \vec{Y}(t)| \tag{28}$$

$$\vec{Y}(t+1) = \vec{Y}_{p_t} - \vec{A} \cdot \vec{D} \tag{29}$$

whereas $\vec{A}$ and $\vec{C}$ indicates the coefficient vectors that are computed using eq (28) and eq (29), t indicates the current iteration $\vec{Y}_{p_t}$ and $\vec{Y}$ indicates the position of prey and grey wolf respectively.

$$\vec{A} = 2\vec{a} \cdot \vec{r}_1 - \vec{a}_1 \tag{30}$$

$$\vec{C} = 2 \cdot \vec{r}_2 \tag{31}$$

Here, $\vec{a}$ indicates a variable, whereas, $\vec{r}_1$ and $\vec{r}_2$ indicates the arbitrary vectors, is stated in eq (30) and (31) [13].

Usually, the hunt is a guide based on the social hierarchy. The hunting nature can be scientifical as stated exploiting the below formulations:

Here, the primary 3 solutions are represented as optimum and remaining solutions are unused, in that state's average of optimal three solutions.

$$\vec{D}_\alpha = |\vec{C}_1 \cdot \vec{Y}_\alpha - \vec{Y}(t)| \quad \vec{D}_\beta = |\vec{C}_2 \cdot \vec{Y}_\beta - \vec{Y}(t)| \tag{32}$$

$$\vec{D}_\delta = |\vec{C}_3 \cdot \vec{Y}_{\delta_=} - \vec{Y}(t)| \quad \vec{Y}_1 = \vec{Y}_\alpha - \vec{A}_1 \cdot (\vec{D}_\alpha)| \; \vec{Y}_2 = \vec{Y}_\beta - \vec{A}_2 \cdot (\vec{D}_\beta)| \tag{33}$$

$$\vec{Y}_3 = \vec{Y}_\delta - \vec{A}_3 \cdot (\vec{D}_\delta)|$$

$$\vec{Y}(t+1) = \frac{\vec{y}_1 + \vec{y}_2 + \vec{y}_3}{3} \tag{34}$$

5.4 Proposed Hybrid Genetic Based GWO

The major inspiration of the proposed method is to integrate the benefits of Genetic Algorithm (GA) [14] in traditional GWO method to overwhelm the static scales chosen issue in GWO. The traditional GWO comprises of arbitrarily chosen control elements $\vec{r}_1$ and $\vec{r}_2$. In proposed model, genetic operators namely: mutations and cross over are comprised to choose optimum control parameters. The information of proposed method is described in subsequent sections.

5.4.1 Generation of Initial Population

The GA and GWO is population based optimization techniques. In proposed technique that produces population comprise of n_1 amount of locations for grey wolfs and n_2 amount of initialized population for Genetic Algorithm. In proposed method, range of n_1 can be “20, 50, 100,200” or any superior values, where range of n_2 is “10, 20, 50” or any slightest values and n_2 must be smaller than n_1 in every iteration.

5.4.2 Optimal Selection

In proposed method, two control parameters such as $\vec{r}_1$ and $\vec{r}_2$ is chosen exploiting genetic operators. The existing Genetic Algorithm possessing static crossover value and mutation as studied in several studies. In proposed method, dynamic mutation ratio and crossover ratio is exploited, that comprise of subsequent three steps: a) rank all the population on the basis of the fitness b) discover average of fitness value and fixed as value of threshold c) abandonment all population by means of smallest amount fitness than value of threshold by means of novel population [13].

5.4.3 Generation of Social Hierarchy

The optimal location is chosen based on the fitness, whereas, $\vec{Y}_\alpha$, $\vec{Y}_\beta$ and $\vec{Y}_\delta$ indicates first, second and third search agents respectively. The flow chart for proposed model is shown in Fig 1.

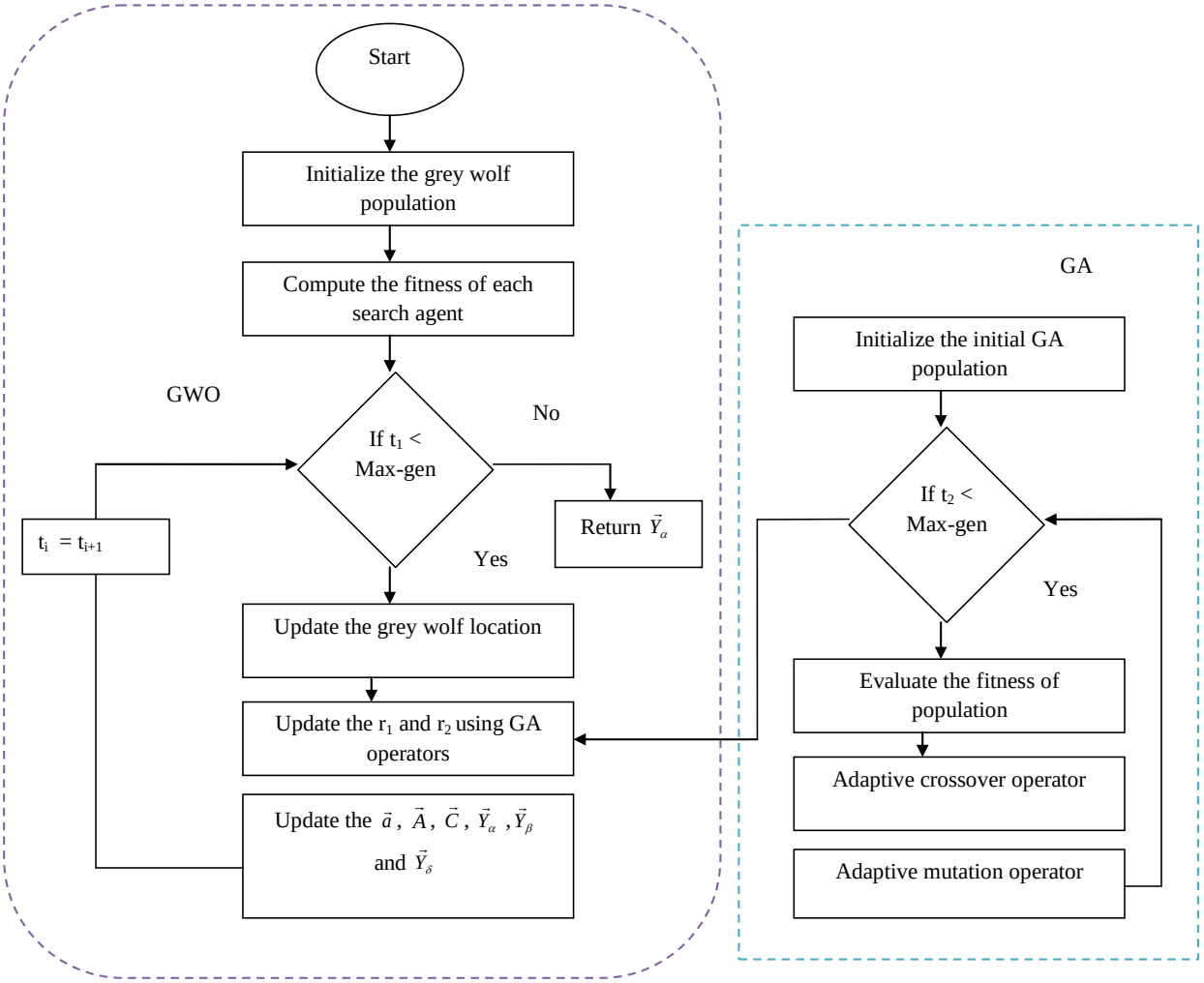

Fig 1: *Process model of proposed GA based GWO model*

6. Results and Discussions

6.1 Experimental Procedure

The proposed brain tumour classification model was experimented by exploiting MATLAB. The dataset exploited for experimentation was obtained from "https://figshare.com/articles/brain_tumor_dataset/1512427". The simulation is performed by using splitting dataset into five test cases. Furthermore, proposed model performance is examined over existing models such as Particle Swarm Optimization (PSO), Firefly (FF), Genetic Algorithm (GA), and Grey Wolf Optimization (GWO) regarding accuracy, specificity, sensitivity, precision, and False Positive Rate (FPR), Net present value (NPV), Negative Predictive Value (NPV), False Positive Rate (FPR), False Discovery Rate (FDR), False Negative Rate (FNR),, F1_score and Matthews correlation coefficient (MCC) metrics.

6.2 Performance Analysis

In this section, the complete analysis of the proposed method with the existing schemes is explained. In Table 1 the proposed method is examined over positive and negative performance metrics. The outcome is demonstrated by means of superior performance of proposed method with the existing models for five test cases.

Table 1: *Statistical Analysis Of Proposed And Existing Models For 5 Test Cases*

			Test case 1			
Measure	GA	FF	PSO	ABC	GWO	Proposed
Accuracy	0.90359	0.90533	0.9085	0.89553	0.9135	0.93158
Specificity	0.98059	0.94549	0.98559	0.98885	0.98559	0.99345
Sensitivity	0.84941	0.88531	0.88551	0.81088	0.88933	0.88951
Precision	0.93899	0.91955	0.95058	0.94448	0.95153	0.98158
FNR	0.33039	0.31549	0.33559	0.38933	0.31088	0.33059
FPR	0.039513	0.035315	0.03551	0.013355	0.03551	0.008353
FDR	0.081004	0.08054	0.059535	0.033333	0.05858	0.018519
NPV	0.98059	0.94549	0.98559	0.98885	0.98559	0.99345
F1_score	0.85183	0.85454	0.85954	0.81931	0.85848	0.84885
MCC	0.88055	0.88388	0.89335	0.84553	0.80338	0.83594
			Test case 2			
Measure	GA	FF	PSO	ABC	GWO	Proposed
Accuracy	0.89553	0.88335	0.88889	0.89314	0.89389	0.9135
Specificity	0.94335	0.95343	0.95098	0.98539	0.95833	0.9951
Sensitivity	0.8598	0.8598	0.84581	0.80588	0.84581	0.85
Precision	0.91184	0.88089	0.88434	0.94	0.90183	0.9881
FNR	0.3503	0.3503	0.33539	0.39513	0.33539	0.35
FPR	0.034845	0.054383	0.05903	0.015804	0.051448	0.005903
FDR	0.088335	0.13931	0.11345	0.05	0.098344	0.013903
NPV	0.94335	0.95343	0.95098	0.98539	0.95833	0.9951
F1_score	0.83888	0.81153	0.83105	0.81354	0.83859	0.85338
MCC	0.84098	0.83015	0.85534	0.85858	0.85493	0.80848
			Test case 3			
Measure	GA	FF	PSO	ABC	GWO	Proposed
Accuracy	0.89804	0.90033	0.90033	0.89314	0.89849	0.91013
Specificity	0.95588	0.95588	0.95588	0.98539	0.95588	0.99345
Sensitivity	0.88951	0.88933	0.88933	0.80588	0.88531	0.8551
Precision	0.89831	0.89955	0.89955	0.94	0.89888	0.98045
FNR	0.33059	0.31088	0.31088	0.39513	0.31549	0.3559
FPR	0.055118	0.055118	0.055118	0.015804	0.055118	0.008353
FDR	0.10149	0.10054	0.10054	0.05	0.10113	0.019355
NPV	0.95588	0.95588	0.95588	0.98539	0.95588	0.99345
MCC	0.8455	0.88313	0.88313	0.85858	0.84831	0.8998
F1_score	0.83545	0.85083	0.85083	0.81354	0.8388	0.8548
			Test case 4			
Measure	GA	FF	PSO	ABC	GWO	Proposed
Accuracy	0.89553	0.90194	0.89849	0.90194	0.89849	0.9135
Specificity	0.95588	0.94335	0.95353	0.9951	0.95833	0.99855
Sensitivity	0.88551	0.88951	0.88933	0.81549	0.88951	0.8551
Precision	0.89883	0.91389	0.89555	0.98459	0.90351	0.99354
FPR	0.055118	0.034845	0.054549	0.005903	0.051448	0.003551
NPV	0.95588	0.94335	0.95353	0.9951	0.95833	0.99855
FNR	0.33559	0.33059	0.31088	0.38531	0.33059	0.3559
FDR	0.10338	0.084308	0.10554	0.013515	0.094591	0.004534
F1-score	0.83158	0.85138	0.83855	0.83955	0.83485	0.85155
MCC	0.84048	0.8841	0.84833	0.88353	0.84835	0.80859
			Test case 5			
Measure	GA	FF	PSO	ABC	GWO	Proposed
Sensitivity	0.84941	0.8598	0.84581	0.83559	0.84581	0.8559
Accuracy	0.89553	0.89314	0.89553	0.90359	0.89804	0.9135
Precision	0.9033	0.90114	0.90498	0.98013	0.91338	0.98089
Specificity	0.95833	0.95833	0.94088	0.99345	0.94335	0.99345
FNR	0.33039	0.3503	0.33539	0.38551	0.33539	0.3551
FPR	0.051448	0.051448	0.039314	0.008353	0.034845	0.008353
FDR	0.098801	0.098838	0.093033	0.019848	0.088819	0.019108
NPV	0.95833	0.95833	0.94088	0.99345	0.94335	0.99345
MCC	0.84083	0.85313	0.84083	0.88534	0.84584	0.80493
F1_score	0.83049	0.83558	0.83989	0.8338	0.833	0.85319

7. Conclusion

This work introduced a novel method for classification of brain tumors. The estimate procedure was done in 5 states like "(i) denoising, (ii) skull stripping, (iii) segmentation, (iv) feature extraction and (v) classification". Initially, denoising procedure was employed and skull stripping procedure was performed by using the morphology segmentation and Otsu thresholding. The subsequent phase subsequent to skull stripping was segmentation and done by using Adaptive CLFAHE model. Next, the feature extraction was performed by exploiting the GLCM. The concluding phase was classification and it was hold by exploiting the hybridized algorithm (naive Bayes classifier and FNN). The most important aim of this article was chosen of hidden neurons in FNN and bounds in fuzzy was chosen optimally by exploiting novel hybrid GA and GWO. Ultimately, the proposed method was examined over the existing algorithms regarding the negative and positive performance measures.

References

[1] M B naceur, Mohamed Akil, Rachida Saouli, Rostom Kachouri,"Fully automatic brain tumor segmentation with deep learning-based selective attention using overlapping patches and multi-class weighted cross-entropy", Medical Image Analysis, Volume 63, July 2020.

[2] Mohamed A. Naser, M. Jamal Deen,"Brain tumor segmentation and grading of lower-grade glioma using deep learning in MRI images", Computers in Biology and Medicine,Volume 121, June 2020.

[3] P. M. Siva Raja, Antony Viswasa rani, "Brain tumor classification using a hybrid deep autoencoder with Bayesian fuzzy clustering-based segmentation approach", Biocybernetics and Biomedical EngineeringVolume 40, Issue 1January–March 2020, Pages 440-453.

[4] Arti Tiwari, Shilpa Srivastava, Millie Pant,"Brain tumor segmentation and classification from magnetic resonance images: Review of selected methods from 2014 to 2019", Pattern Recognition Letters, Volume 131, March 2020, Pages 244-260.

[5] Fatih ŞİŞİK, Eser SERT,"Brain tumor segmentation approach based on the extreme learning machine and significantly fast and robust fuzzy C-means clustering algorithms running on Raspberry Pi hardware", Medical Hypotheses,Volume 136, March 2020.

[6] Zexun Zhou, Zhongshi He, Yuanyuan Jia," AFPNet: A 3D fully convolutional neural network with atrous-convolution feature pyramid for brain tumor segmentation via MRI images",Neurocomputing,Volume 40218, August 2020, Pages 235-244.

[7] H. Chang, "Entropy-based trilateral filtering for noise removal in digital images," 2010 3rd International Congress on Image and Signal Processing, Yantai, 2010, pp. 673-677.

[8] Yousefi, Jamileh, "Image Binarization using Otsu Thresholding Algorithm", 2015.

[9] Chris EbeyHoneycutt, RoyPlotnick,"Image analysis techniques and gray-level co-occurrence matrices (GLCM) for calculating bioturbation indices and characterizing biogenic sedimentary structures", Computers & Geosciences, vol.34, no.11, pp.1461-1472, November 2008.

[10] Ms. Asha, Mr. Krishan Gupta," A Basic Approach to Enhance a Gray Scale Image", Imperial Journal of Interdisciplinary Research (IJIR), vol.2, no.7, 2016.

[11] Kayri, Murat,"Predictive Abilities of Bayesian Regularization and Levenberg–Marquardt Algorithms in Artificial Neural Networks: A Comparative Empirical Study on Social Data", Mathematical and Computational Applications, 2016.

[12] E. Daniel, J. Anitha and J. Gnanaraj "Optimum laplacian wavelet mask based medical image using hybrid cuckoo search – grey wolf optimization algorithm", Knowledge-Based Systems vol. 131, no. 1, pp. 58–69, Sep. 2017.

[13] E.Daniel, J. Anitha, "Optimum green plane masking for the contrast enhancement of retinal images using enhanced genetic algorithm", Optik 126 (2015) 1726–1730.

[14] J. Li, Z. Peng, Multi-source image fusion algorithm based on cellular neural networks with genetic algorithm, Optik 126 (2015) 5230–5236.

[15] V. Nair , G.E. Hinton , "Rectified linear units improve restricted Boltzmann ma- chines", in: Proceedings of International Conference on Machine Learning, 2010, pp. 26–30.

[16] Quazi M. H and Dr. S. G. Kahalekar,"Artifacts Removal using Dragonfly Levenberg Marquardt-Based Learning Algorithm from Electroencephalogram Signal"Multimedia Research, Volume 2, Issue 2, April 2019.

[17] V. Vinolin,"Breast Cancer Detection by Optimal Classification using GWO Algorithm"Multimedia Research, Volume 2, Issue 2, April 2019.

[18] R. Cristin,Dr.V.Cyril Raj and Ramalatha Marimuthu,"Face Image Forgery Detection by Weight Optimized Neural Network Model,"Multimedia Research, Volume 2, Issue 2, April 2019.

[19] Vinusha S.,"Secret Image Sharing and Steganography Using Haar Wavelet Transform"Multimedia Research, Volume 2, Issue 2, April 2019.